energies

MDPI

Article

Evaluation of an Energy Separation Device for the Efficiency Improvement of a Planar Solid Oxide Fuel Cell System with an External Reformer

Jinwon Yun [1], Eun-Jung Choi [2], Sangmin Lee [2,*], Younghyeon Kim [3] and Sangseok Yu [3,*]

[1] Department of Hydrogen System Engineering, Youngsan University, Yangsan-si 50510, Republic of Korea; jwyun@ysu.ac.kr
[2] Department of Zero-Carbo Fuel & Power Generation, Korea Institute of Machinery and Materials, Daejeon 34103, Republic of Korea
[3] Department of Mechanical Engineering, Chungnam National University, Daejeon 34134, Republic of Korea
* Correspondence: victlee@kimm.re.kr (S.L.); sangseok@cnu.ac.kr (S.Y.); Tel.: +82-42-868-7833 (S.L.); +82-42-821-5646 (S.Y.)

Abstract: Due to the high operating temperature of solid oxide fuel cells (SOFC), the system efficiency depends on efficient thermal integration and the effective construction of system configuration. In this study, nine configurations of system integration design were investigated to evaluate the possible improvement of system efficiency with energy separation devices. The models were developed under the Matlab/Simulink® platform with Thermolib® module. The reference layout of the simulation included an SOFC stack, a compressor, an external reformer with a burner, a three-way valve, a heat exchanger, and a water pump. From the reference case, eight cases extended layouts for the capability of thermal energy utilization with a catalytic converter, SOFC hybridization, and an energy separation device. Since the energy separation device was beneficial to thermal energy utilization via a boost to the gas temperature, electric efficiency, and combined heat and power (CHP) efficiency was improved with the thermal integration of the energy separation device with a turbo generator.

Keywords: solid oxide fuel cell; energy separation device; electric efficiency; CHP efficiency

check for updates

Citation: Yun, J.; Choi, E.-J.; Lee, S.; Kim, Y.; Yu, S. Evaluation of an Energy Separation Device for the Efficiency Improvement of a Planar Solid Oxide Fuel Cell System with an External Reformer. *Energies* **2023**, *16*, 3947. https://doi.org/10.3390/en16093947

Academic Editor: Jurgita Raudeliūnienė

Received: 23 March 2023
Revised: 1 May 2023
Accepted: 2 May 2023
Published: 8 May 2023

Copyright: © 2023 by the authors. Licensee MDPI, Basel, Switzerland. This article is an open access article distributed under the terms and conditions of the Creative Commons Attribution (CC BY) license (https://creativecommons.org/licenses/by/4.0/).

1. Introduction

Worldwide climate change drives the development of alternative power sources and the efficiency improvement of conventional power plants. A solid oxide fuel cell (SOFC) is an attractive alternative to a conventional power plant due to high efficiency, the toxic free exhaust gas, a variety of fuel options, modularity, low noise, and possible mass production capability [1]. Additionally, the high-temperature exhaust gas from the SOFC system could be an optional advantage for a Combined Heat and Power (CHP) system.

At present, a solid oxide fuel cell has been developed in many different types, such as internally reforming or externally reforming, bottoming cycle or tri-gen cycle, planar, tubular, or circular shapes. The variety of different system developments were inspired by different motivations, but the common factor is the improvement of system efficiency with reliability.

In contrast to the low-temperature fuel cell systems, the efficiency of SOFC systems strongly depends on thermal energy utilization. The thermal energy of SOFC is generated by electrochemical reactions of fuel cells and heat release from the catalytic combustion of fuel lean anode-off gas. A portion of the thermal energy is provided for the SOFC stack to maintain the temperature, but most is exhausted from the stack and catalytic burner. Many options for thermal energy utilization are reported, such as anode gas recycling, cathode gas recycling for reducing parasitic power, and the heating of anode gas and cathode gas by exhaust gas. This type of energy saving is very similar to the regeneration of conventional power plants.

Hybrid power generation with turbo-machinery is an attractive advantage of SOFC that can improve efficiency due to the high-temperature exhaust gas of SOFC [2–5]. The combined hybrid cycle has high efficiency when the capacity of a power plant is very large. Currently, system research into SOFC is focused on the internally reforming SOFC [6,7], which has advantages of directly utilizing thermal energy from electrochemical heat generation in an endothermic steam reforming reaction. However, since the carbon deposition of the internal reforming reaction is critical for long-term operation, the internal reforming SOFC is limited in operating flexibility. It should also be noted that internal reforming SOFC has a vast temperature difference between the inlet and outlet [8], which harms durability and performance. On the other hand, the external reforming SOFCs were free from carbon deposition on the surface of the SOFC channel. The temperature gradient of external reforming SOFC is narrow, which is suitable for large stationary power plants. It is emphasized that the variety of thermal energy utilization is another advantage of external reforming SOFC [9].

External reforming SOFCs show attractive benefits for central power generation systems. Nevertheless, it is still necessary to design a proper thermal utilization concept to improve system performance. A few layout studies of SOFCs have been reported [10–12] regarding the hybrid configuration of power plants. Saebea et al. analyzed the performance of SOFC external reform, which integrated an external biogas reformer. The results showed that the system using ethanol as fuel in the external reforming of SOFC had the highest electrical and thermal efficiency [13]. Saebea et al. also reported a cycle analysis of an external reforming SOFC system with a gas turbine that effectively improved system efficiency with optimal thermal utilization [14]. S. Ma et al. presented an external reforming SOFC with bioethanol fuel as a vehicle energy source. The system efficiency was approximately 44.4% at the design point, which maximizes the utilization of wasted thermal energy [15]. Deng et al. reported an SOFC system with a methane steam reforming system to produce hydrogen with electricity. They showed the proper operating temperature to run an SOFC system with methane steam reforming that was specialized for hydrogen production [16].

Even though external reforming SOFC has strengths of durability and stability, the system efficiency of the external reforming SOFC is still not satisfactory for stationary power plants. In particular, the conventional burner provides various options for system layouts, but harmful gas emissions limit the utilization of the conventional burner for SOFC. When thermal energy utilization is conducted with a catalytic burner, a low maximum operating temperature of the catalytic burner also limits the system efficiency. In this study, nine configurations of SOFC systems were established to study the system efficiency of planar-type SOFC systems with external reformers. The simulation model was developed under Thermolib® with Matlab/Simulink platform. The exhaust gas temperature of each layout was tuned to be the same for comparison. A new idea in this study is the evaluation of the feasibility of an energy separation device for efficiency improvement. Firstly, the conventional approach to thermal energy utilization is studied. Then, it is extended to the various regeneration configurations with an energy separation device. The optimal system is finally suggested via various configurations.

2. A Simulation of the SOFC Hybrid System

2.1. A Description of the Fuel Cell Components Model

The planar SOFC possesses a higher power density than the tubular type SOFC because it has higher performance and a shorter path for current flows in the thorough plane direction. Braun et al. [17] showed that an external reforming SOFC performed better than an internal reforming SOFC in stack efficiency. The advantage of an external reforming stack is to utilize the thermal energy of the system very effectively.

This study evaluates performance improvements via various combinations of thermal energy utilization modules with SOFC. The chemical reactions of the SOFC stack at both electrodes are as follows [17]:

$$\text{Anode}: \ H_2 + O^{2-} \rightarrow H_2O + 2e^- \tag{1}$$

$$\text{Cathode}: \ \frac{1}{2}O_2 + 2e^- \rightarrow O^{2-} \tag{2}$$

$$\text{Overall}: \ H_2 + O_2 \rightarrow H_2O \tag{3}$$

The electrochemical reactions of Equations (1)–(3) generate electricity as well as heat. The outlet concentrations of gas species at anode and cathode channels are calculated by stack module.

The simulation model is constructed using Thermolib® R5.4, which is a simulation tool box of thermodynamic systems in MATLAB®/Simulink®. Figure 1 shows the SOFC system simulation model developed in this study. In the Thermolib Toolbox, the SOFC stack block requires information on cell voltage, current density, and operating temperatures. The SOFC stack toolbox requires a polarization curve to determine the electricity with thermal energy. Braun et al. presented the performance curve of the SOFC stack with reformed gases. The reformed gas comprised 65.4% H_2, 14.5% CO, 5.4% CO_2, and 14.6% H_2O. The polarization curve is shown in Figure 2 [17].

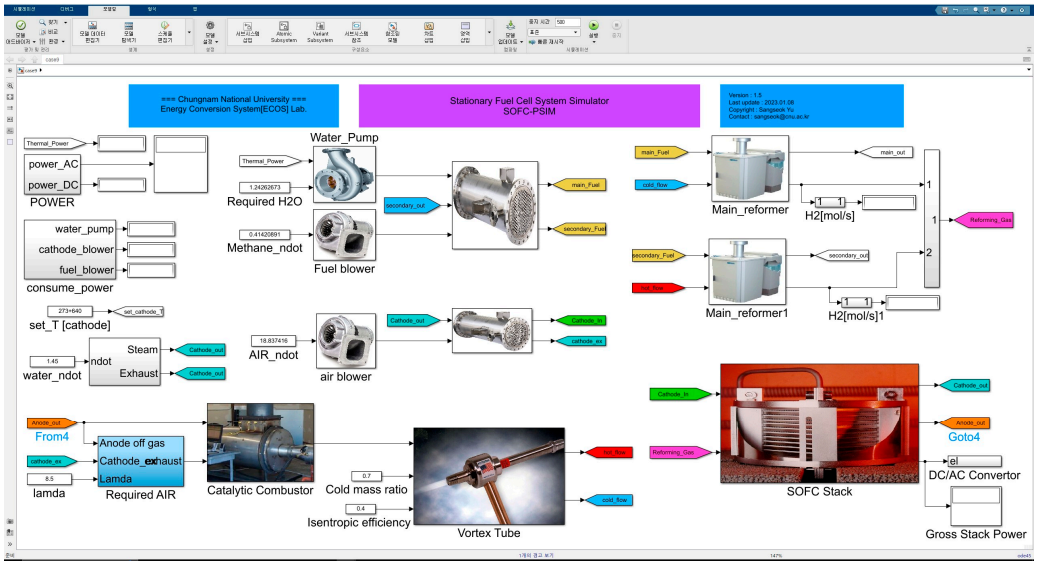

Figure 1. SOFC System Simulation Model via Thermolib® under Simulink® Platform.

Based on single-cell voltage, the fuel cell stack was assumed to be the series connection of a single cell that satisfies power requirements. Additionally, the cell-to-cell variation of the fuel cell stack was neglected. The active area of the SOFC was 250 cm^2, and the fuel utilization factor was 85%. The operating pressure of the stack was set to 1 bar.

The steam reformer was modeled using an equilibrium reactor that calculated equilibrium compositions at a given temperature and pressure. The operating temperature of the reformer ranged from 800 °C to 850 °C. The equilibrium reaction comprised two elementary reactions: the steam reforming reaction in Equation (4), and the water gas shift reaction in Equation (5).

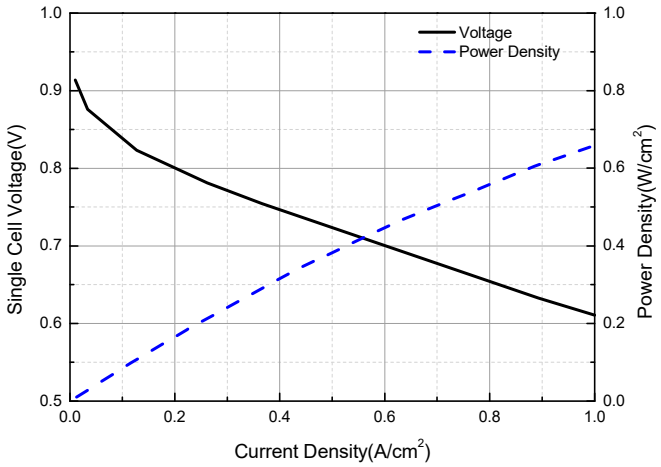

Figure 2. Polarization curve of solid oxide fuel cell at 800 °C [17].

$$CH_4 + H_2O \rightarrow CO + 3H_2 \ [\Delta H = 206 \text{ kJ/mol}] \quad (4)$$

$$CO + H_2O \rightarrow CO_2 + H_2 \ [\Delta H = -41 \text{ kJ/mol}] \quad (5)$$

The equilibrium reactor is required to absorb thermal energy from the heat source. The heat source of the reforming reactor can be the heat of the electrochemical reaction or the heat of combustion from the burner. The heat transfer performance of the reforming reactor is determined by the flow arrangement of hot and cold gas, internal gas passes, and materials. In this study, the equilibrium reactor was assumed to be a shell and tube packed-bed reactor with a geometric structure, as reported by Ghang [18].

The effective heat transfer coefficient of the gas in the packed bed is shown in Figure 3. The effective heat transfer coefficient profile was used to determine the heat transfer rate from burner to reformer. It also investigated the equilibrium composition of the reformer over pressure increase.

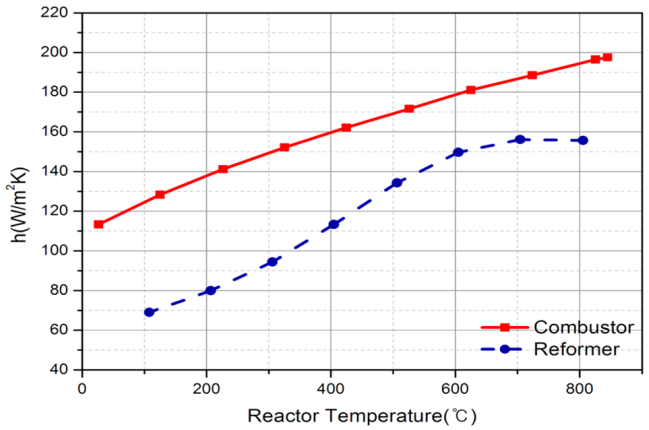

Figure 3. Heat transfer coefficients in the external reformer with a catalytic combustor [18].

Figure 4 shows the reformed gas composition in terms of temperature and pressure, as calculated by the thermodynamic equilibrium reaction. As the reaction pressure increased, the hydrogen conversion rate was reduced and the methane flow rate increased in the equilibrium reaction because the backward reaction of the reforming reaction was more accelerated. Consequently, more fuel had to be supplied for the reformer and combustor to supply the hydrogen needed to the stack than in the ambient pressure SOFC system. Additionally, it is known that the reformer temperature increased.

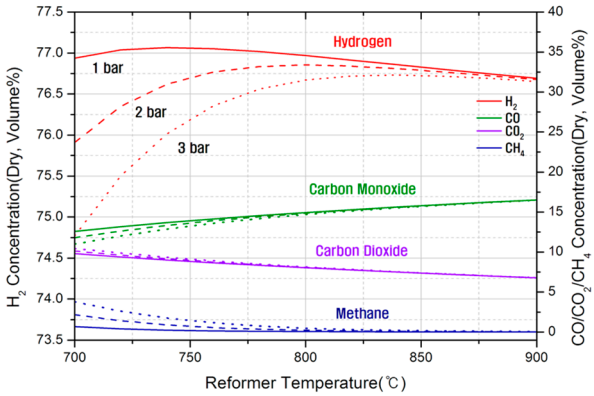

Figure 4. Reformed gas composition in terms of system pressures.

The thermal efficiency of the SOFC system depends on the effective utilization of wasted thermal energy. In an external reforming planar solid oxide fuel cell system (ERP-SOFC), additional fuel provided to the burner activated the endothermic methane steam reforming reaction. Since the reformer was heated by the heat release of extra fuel to maintain the stability criteria of a practical system, the system efficiency of the ERP-SOFC system was severely affected by the amount of fuel addition. The additional fuel supply for the burner of the steam reformer lowered the system efficiency of the ERP-SOFC. When the burner of the external reformer was replaced with another component or the method of heat supply to the reformer was changed, the system efficiency could be improved.

In this study, the burner was fueled by the anode-off gas from the stack that had a number of fuel gases. Since the anode-off gas contained a higher concentration of inert gases, such as CO_2 and H_2O, the fuel concentration at the anode exit was lean. Hence, the flammability of the anode-off gas was very limited. For the comparison, two types of combustors were modeled: one for a conventional burner, and the other for a catalytic combustor.

A catalytic combustor was applied to burn out the anode-off gas no matter the operating ranges [19]. The model of a catalytic combustor was an equilibrium reactor with an operating temperature lower than the conventional combustor. The operating temperature of the catalytic combustor was controlled by an excess air flow rate from 850 °C to 900 °C, while the conventional combustor was operated from 1200 °C to 1300 °C. The total methane consumption rate and steam power were calculated by the assumption of an equilibrium reaction, as shown in Table 1.

Table 1. Amount of fuel energy for the SOFC system (reference system).

Index	Fuel Type and Unit	Description
Reformer	Methane (kW)	336.7
Burner	Methane (kW)	134.7
Stack	Reformed hydrogen (kW)	334.0

A turbine and a compressor were modeled thermodynamically. The isentropic efficiency of the device was set to 80%, and the turbine inlet temperature ranged from 500 °C to 800 °C depending on the operating conditions of the SOFC system.

Other balance of plant (BOP) components were a heat exchanger, three-way valve, PID controller, pump, compressor, and mixer. A heat exchanger was modeled as a counter-flow gas-to-gas heat exchanger. Pressure drops through the components were assumed to be negligible. The three-way valve and PID controller were used to control the temperature and flow rate, which was used to control the airflow rate into the cathode side. The compressor provided the airflow to the cathode side and combustor, while the water pump supplied the water to the reformer.

2.2. Temperature Rise with the Energy Separation Device

The energy separation device is known as a vortex tube, which is a device to separate the inlet gas into the hot exhaust gas and cold exhaust gas. The principle of a vortex tube is to separate induced mass and energy by the generation of vortices and the Joule–Thomson effect, so that the temperature and mass separation can be observed at the cold and hot gas exits. A vortex tube comprises a vortex generator, a main tube, a hot flow control valve, and a cold flow orifice.

This study considered the vortex tube as an auxiliary device to evaluate system efficiency improvement. The model was developed with mass and energy conservation inside the vortex tube and energy separation characteristics, as follows. The following terms were utilized to evaluate the performance of the vortex tube.

$$\text{Hot temperature difference}: \ \Delta T_h = T_h - T_{in} \tag{6}$$

$$\text{Cold temperature difference}: \ \Delta T_c = T_{in} - T_c \tag{7}$$

$$\text{Isentropic temperature difference}: \ \Delta T_{is} = T_{in} - T_{is} = T_{in}\left[1 - \left(\frac{p_a}{p_{in}}\right)^{((\gamma-1)/\gamma)}\right] \tag{8}$$

$$\text{Isentropic efficiency}: \ \eta_{is} = \frac{\Delta T_c}{\Delta T_{is}} \tag{9}$$

$$\text{Cold mass ratio (or cold mass fraction)}: \ \varepsilon = \frac{\dot{m}_c}{\dot{m}_{in}} \tag{10}$$

Even if a vortex tube is a possible candidate for efficiency improvement, it will be necessary to determine the optimal combination with various BOPs. This study considered various layouts for the optimum combination of the vortex tube with other components. The flow rate of the vortex tube at the hot-fluid exit was maximized when the cold mass ratio was 0.7–0.8 [20–25]. The isentropic efficiency of the vortex tube was set to 30%, the cold mass ratio was 70%, ΔT = 50 °C, and the operating pressure was 2 bar.

2.3. Net Power and Efficiency of the SOFC System

The net power of the SOFC system is calculated as follows:

$$P_{net} = \left(P_{gross} \times \eta_{inverter}\right) - \sum P_{BOP} \tag{11}$$

where P_{gross} is stack output power, P_{BOP} is the power consumption of the *BOP* component, and $\eta_{inverter}$ is the efficiency of the inverter (DC to AC).

The electric efficiency of an ERP-SOFC system is defined as the net power output to grid divided by energy input. Therefore,

$$\eta_{sys,elec} = \frac{P_{AC,net} + P_{turb}}{\left(\dot{n}_{fuel} \times LHV_{fuel}\right)_{sys,in}} \tag{12}$$

where $\dot{n}_{fuel}$ (mol/s) is the molar flow rate of total fuel into the system, LHV_{fuel} (kJ/mol) is the lower heating value of fuel, and P_{turb} (kW) is the turbine power out.

The thermal efficiency of the ERP-SOFC system is defined by the net power output and thermal energy to the grid divided by energy input.

$$\eta_{sys,CHP} = \frac{P_{AC,net} + P_{Turb} + \dot{Q}_{thermal}}{\left(\dot{n}_{fuel} \times LHV_{fuel}\right)_{sys,in}} \tag{13}$$

where $\dot{Q}_{thermal}$ (kW) is the thermal energy to the grid.

In Table 2, the parameters are summarized. The exit gas temperature was set to 130 °C, which was exhausted to the atmosphere.

Table 2. Simulation parameters of the SOFC cycle calculation.

Index	Parameters	Description
FC stack	Number of cells in SOFC stack	2105
	Electro-active area (cm^2)	250
	Current density (A/cm^2)	0.38
	Cell voltage (V)	0.75
	Power density (W/cm^2)	0.285
	SOFC fuel utilization (%)	75
	SOFC air utilization (%)	14.4 ± 0.4
	Operating cell temperature (°C)	800
	Cathode temperature rise (°C)	180
Reformer	Steam-to-carbon ratio	3
	Reforming temperature (°C)	800
BOPs	Air compressor efficiency (%)	80
	Fuel compressor efficiency (%)	80
	Pump efficiency (%)	65
	Turbine efficiency (%)	80
	Vortex tube efficiency (%)	30
	Steam separator efficiency (%)	80
	Inverter efficiency (%)	95
Fuel Condition	Fuel type	CH_4
	LHV (kJ/kg)	50,010

2.4. System Layouts for the Case Study

This study evaluates various configurations of SOFC systems to find the maximum efficiency with external reforming SOFC systems. The cases start from the reference case, which has core components, and then the cases are extended from the reference cases. Table 3 shows the cases of the configuration study.

Table 3. Description of the SOFC System Configuration.

Case No.	Descriptions
Case 1	Reference case
Case 2	Replacement of conventional burner with catalytic burner (anode off-gas)
Case 3	Reference case with turbine at the exit of burner
Case 4	Case 2 with turbine at the exit of catalytic burner
Case 5	Case 1 with vortex tube at the exit of burner
Case 6	Case 2 with vortex tube at the exit of catalytic burner
Case 7	Case 3 with vortex tube
Case 8	Case 4 with vortex tube
Case 9	Case 8 with secondary reformer

Table 4 is shown in Figure 4. Case 1 in Figure 4 is a reference layout composed of the SOFC stack, an external reformer with a conventional combustor, a heat exchanger, a PID controller, a three-way valve, a mixer, a compressor, a pump, and an inverter. The hot exhaust gas from the conventional combustor heats up the water for the external reformer. The hot exhausted gas from the catalytic combustor was used to heat up the cathode inlet air. In Case 1, the three-way valve was feedback-controlled to maintain the cathode air inlet temperature. The high-temperature combusted gas from the reformer burner and the exhaust gas from the anode were used to utilize the thermal energy. The

reformer was heated by the external combustor, and anode-off gas was burnt out by the catalytic combustor.

Table 4. Summary of simulation results.

	Unit	Case 1	Case 2	Case 3	Case 4	Case 5	Case 6	Case 7	Case 8	Case 9
Air utilization	%	14.4	14.6	14.4	14.8	14.4	14.4	14	14.6	14
Excess Burner		2.7		2.7		2.8		2.6		5.7
air (λ) Catalytic Combustor			7		6.5		7	9.3	7	5.7
Fuel supply (CH_4)	kg/h	33.93	24.23	33.93	24.23	33.93	24.23	33.93	24.23	28.35
Fuel for burner	kW	134.6	-	134.6	-	134.6	-	134.6	-	57.2
Total fuel	kW	471.3	336.7	471.3	336.7	471.3	336.7	471.3	336.7	393.9
Anode inlet	K	1031	1028	1034	1031	1025	1033	1052	1033	1063
Anode outlet	K	1076	1077	1076	1071	1075	1078	1075	1079	1076
Cathode inlet	K	892	893	894	882	894	893	895	892	894
Cathode outlet	K	1076	1077	1076	1071	1075	1078	1075	1079	1076
Reformer inlet		554	738	510	689	547	766	715	692	668
Burner exit	K	1483	-	1485	-	1462	-	1520	-	1457
Catalytic combustor exit	K	-	1122	-	1128	-	1122	1147	1125	1102
Gas turbine Inlet	K	-	-	770	888	-	-	1075	898	1029
SOFC stack power (DC)	kW	150.6	150.5	150.7	150.7	150.4	150.4	151.1	150.7	151.1
Air compressor	kW	40.63	40.07	40.63	39.53	40.63	40.63	41.79	40.07	41.78
Fuel compressor	kW	1.36	0.97	1.36	0.97	1.36	0.97	1.36	0.97	1.14
Water pump	kW	0.35	0.35	0.35	0.35	0.35	0.35	0.35	0.35	0.35
Parasitic power of BOPs	kW	41.99	41.05	41.99	40.51	41.99	41.61	43.16	41.39	42.92
Net power (AC)	kW	101.1	101.9	101.2	102.7	100.1	101.8	100.4	101.8	100.6
Turbine power	kW	-	-	25.3	77.8	-	-	130.3	86.3	89.8
Thermal power	kW	81.3	106.3	56.4	29.3	79.8	95.3	105.1	24.5	145.9

One way to improve the efficiency is to reduce the extra fuel by replacing the heating technology of the steam reformer. In Case 2, from Figure 5b, a catalytic combustor was utilized instead of a conventional burner to heat up the reformer [15]. Accordingly, the overall fuel consumption was reduced by employing the catalytic combustor directly to heat up the external reformer. When the catalytic combustor was applied to the burn-out of anode from the gas, the maximum exhaust gas temperature was limited due to the durability of the catalyst. Accordingly, the reduction in the burner exit gas availability must be analyzed.

Another way to improve the performance is to combine the fuel cell system with a conventional power plant. Case 3 of Figure 5c showed a similar configuration to Case 1. Nevertheless, the difference was the utilization of the exhaust gas from the anode off-gas combustor in the turbine operation to generate more electricity. Case 4 of Figure 5d had the same configuration as Case 2, except for the turbine. Those cases are typical turbine applications of the fuel cell exhaust gas.

The idea of a vortex tube is to separate the temperature of the inlet gas into higher and lower temperatures and separate the mass flow rate. Even though the catalytic combustor is representative of purity exhaust gases, its operating temperature limits the system efficiency. The configuration layouts from Case 5 to Case 9 are used to confirm the feasibility of the vortex tube in fuel cell applications. When the vortex tube is set up, the inlet flow into the vortex tube is separated into higher- and lower-temperature bodies. Higher temperature gas must have higher availability, and the lower can be used to heat up inlet gases.

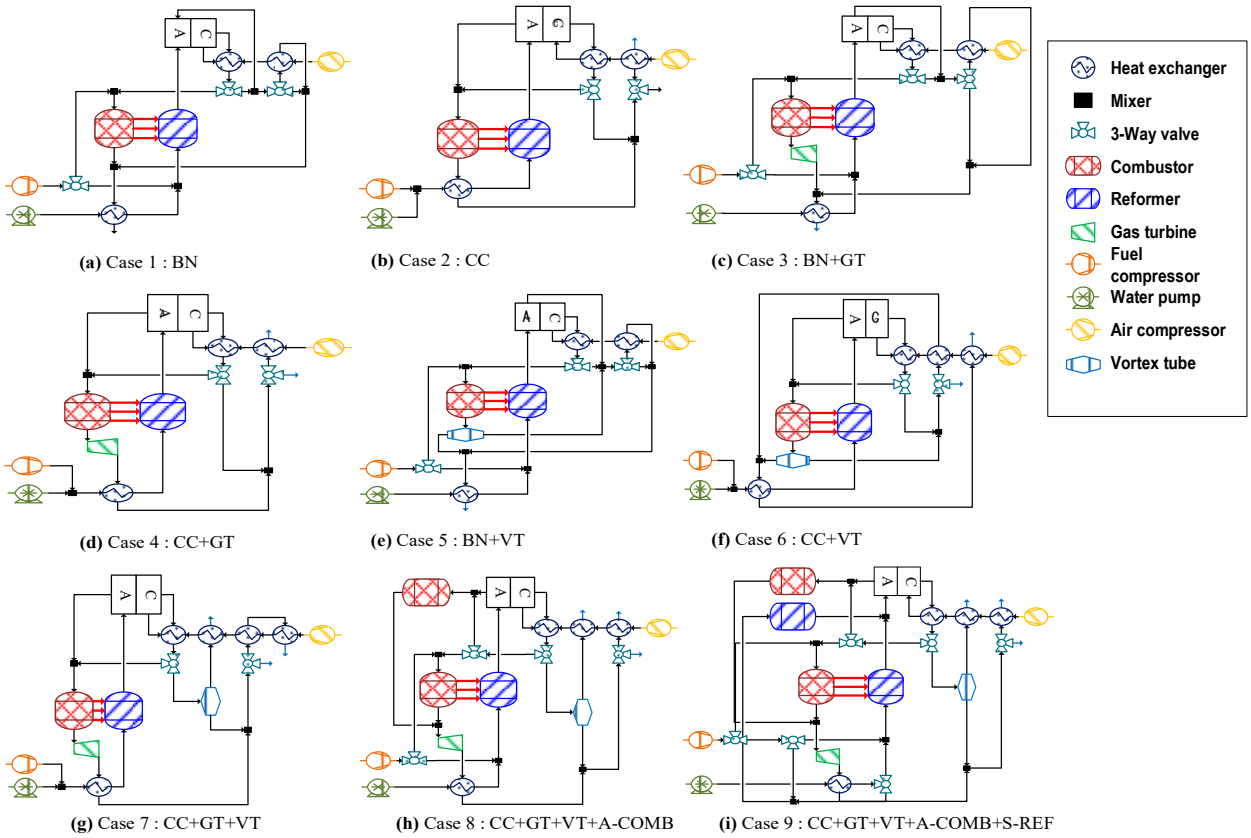

Figure 5. Schematic diagrams of SOFC system layout (CC: Catalytic Combustor, S-Ref: Secondary reformer, BN: Burner, GT: Gas Turbine, VT: Vortex Tube, A-Comb: Additional Combustor).

First, the vortex tube was installed to increase the temperature of the cathode airflow, which is shown in Case 5 and Case 6. A conventional burner was used to heat up the reformer in Case 5, and a catalytic burner was installed in Case 6. In Case 5 (Figure 5e) and Case 6 (Figure 5f), the basic improvements without the extra production of electricity can be observed. In Case 7, in Figure 5g, the vortex tube was applied for preheating the air for the cathode side. Case 7 was a modification of Case 4, so the cathode air was preheated by a vortex tube. Case 8 in Figure 5h modified Case 3, in which the turbine, catalytic combustor, and vortex tube were installed. By doing this, the high temperature and higher flow rate of combusted gas were introduced to the turbine. In Case 9 in Figure 5i, the secondary reformer was installed to utilize the wasted thermal energy.

2.5. Simulation Strategy

Matlab®/Simulink® is a platform for adopting various toolboxes. The Thermolib® toolbox is a simulation toolbox for thermodynamic analysis with dynamics. The library module is a dynamic module that shows dynamic responses during load follow-up. In this study, the dynamic response delayed the evaluation of various evaluation layouts. However, three-way valves were installed in the system that could control the gas flow to maintain the temperature of each component.

When the system efficiency was evaluated, the same reference conditions ought to be considered. The reference condition was the exhausted gas temperature maintained at 130 °C. This regulation was managed by three-way valves. While the exhaust gas temperature was easily managed at the reference value, the component temperature was difficult to control. In some layouts, it was more difficult to fix the same temperatures. Accordingly, more margins should be allowed to manage component temperatures. In this study, a maximum 5 K difference was set to be an allowable temperature for the balance of plant components in terms of temperature.

3. Results and Discussion

In the ERP-SOFC system, an air compressor was used to supply the air to the cathode of SOFC. The cathode exit air was supplied to other components that required air. Since the total air flow rate was intended to satisfy the cooling down of the SOFC, the air utilization factor of the fuel cell was from 14 to 14.8, depending on the system configuration. Table 4 shows a summary of the simulation results over nine different configurations. Since each simulation case should satisfy the terminal temperature from the system, the simulation results of each component varied a little bit.

In Table 4, Case 1 is a reference layout that utilized the exhausted thermal energy from the external burner and the catalytic combustor for heating cathode air and water for the reformer. The exhaust gas from the ERP-SOFC system was set to approximately 130 °C, and gas exit temperatures from both electrodes were approximately 800 °C. In Case 2, the anode off-gas was used to heat up the reformer. This approach could save fuel consumption for the burner and increase thermal energy. However, since the operating temperature of the catalytic burner was lower than the conventional burner, the system has to be a massive structure to enhance heat transfer from the catalytic burner to the reforming section.

When the turbine was connected to the exit of the combustor, more electric power was generated by the turbine. Case 3 and Case 4 connected the turbine at the exit of the combustor. For the proper comparison of the catalytic burner with the conventional burner, the pressure ratio of the turbine was set to 2 in all cases. Case 3 was a modification of the Case 1 layout, in that the turbine was installed to the exhaust gas exit of the external burner in Case 1. In the same manner, Case 4 was a modification of Case 2. Due to the gas flow rate to the turbine, Case 4 produced more turbine power than Case 3, but the thermal power of Case 4 was lower than Case 3. Since the external burner was optimized to supply heat energy to the reformer, the turbine inlet temperature was close to 770 K, lowering turbine power. As shown in Table 4, the decrease in turbine power was not proportional to the increase in thermal power.

The inlet temperature of a turbine is crucial to increasing the turbine power. A vortex tube is an energy separation device that divides inlet gas into hotter and colder gas. A higher temperature can be achieved as the vortex tube is connected to components in SOFC. Case 5 and Case 6 evaluated the system performance via a vortex tube. In Case 5, the turbine of Case 3 was replaced with a vortex tube. Since the gas separation of the vortex tube in both exits limited the heating of the cathode air, thermal power was decreased compared to Case 1. The same trend was observed in Case 6. Even though the vortex tube could not improve the performance of SOFC, the aspect of the vortex tube was still very attractive.

In Case 7, Case 8, and Case 9, the catalytic combustor was set up to provide heat to the reformer. The turbine was also installed to generate extra electricity using hot exhaust gas. The vortex tube was also located at the exit of the cathode, since the advantage of the vortex tube was to separate the temperature and mass flow. This combination improved the turbine power and thermal power of Case 7, Case 8, and Case 9. The hot air of the vortex tube in Case 7 was used to heat up the cathode air, and the cold air was mixed with turbine exit air to be exhausted. The air preheating with the vortex tube saved energy to improve the turbine power. The air excess ratio was also slightly increased to maintain the anode air inlet temperature that increased the turbine power. Case 8 employed the catalytic combustor and conventional burner with the turbine and vortex tube. The vortex tube was used to increase the turbine inlet temperature. Accordingly, the turbine inlet temperature increased to 1075 K, and the net power out was 130.3 kW.

Case 9 employed an external reformer with a conventional burner and a secondary reformer with a catalytic combustor, which shared the hydrogen production with the external reformer. This secondary reformer reduced the total fuel consumption rate by 16.42%. However, since the thermal energy from the catalytic combustor supplied the secondary reformer, the turbine inlet temperature was reduced from 1075 K to 1029 K. As a result, 40.48 kW of the turbine outlet power was reduced.

It is possible to evaluate the efficiency of nine configuration cases with calculation results. Figure 6 shows the efficiency comparison of nine configurations. Case 1, Case 3, and Case 5 were similar configurations to those of conventional burners. The electric efficiency of Case 3 was the highest of the three cases. The vortex tube was less effective for this layout. The thermal efficiencies of the three configurations were also very similar, due to the same utilization approaches. When the conventional burner was replaced with the catalytic burner, the unburnt fuel in the anode off-gas was delivered to the reformer so that the burner did not require extra fuel for heating up. Since the turbine power could be generated in Case 4, the electric efficiency of Case 4 was the highest of the three cases (catalytic combustor layouts).

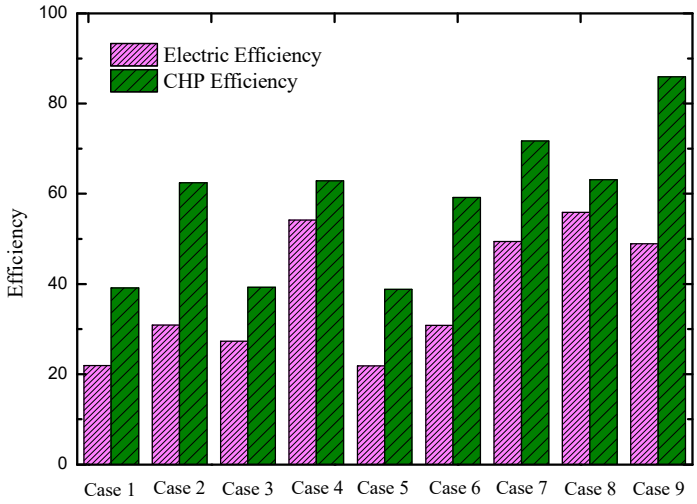

Figure 6. ERPSOFC System Efficiency of nine layouts.

The last three cases, Case 7, Case 8, and Case 9, focused on thermal energy utilization. In Case 7, four heat exchangers were connected to heat up the cathode air. Vortex tubes provided hot gases to one of the heat exchangers, contributing to increasing the cathode air temperature. The CHP efficiency of Case 7 was 71.69%, and the electric efficiency of the SOFC system was 49.4%. The conventional burner of Case 8 and Case 9 had a key role in efficiency improvement. Additionally, three heat exchangers with vortex tubes increased the cathode air temperature. The advantage of a conventional burner is its high-temperature operation, increasing the turbine power. On the other hand, anode off-gas was burnt out with a catalytic burner utilized in the configuration. The maximum electric efficiency in the nine configurations was observed in Case 8, which produced electricity using a fuel cell and turbine. On the other hand, the maximum CHP efficiency was also observed in Case 9.

As shown in Table 4, a conventional burner requires extra fuel to heat up the reformer. Figure 7 shows a power breakdown analysis of various cases. The percentage power of each component was estimated by the percentage ratio of the component power over total power input. Residual gas in Figure 7 means exhausted energy without any utilization. Even though the same amount of power was extracted from the fuel cell stack, the percentage power of the stack was varied due to variations in the total power input. Cases with conventional burners exhausted significant amounts of energy without utilization. Since the catalytic burner induced fuel lean anode off-gas, the additional fuel was not delivered to the catalytic burner, which generated a greater portion of power from the fuel cell stack. It was observed that the turbine power was enlarged as the catalytic burner was integrated. Additionally, the turbine could be maximized as the system integrated the catalytic burner with a vortex tube, which is shown in Cases 7, 8, and 9. Hence, it is shown that the temperature increase capability of energy separation devices contributes to improving the turbine power output.

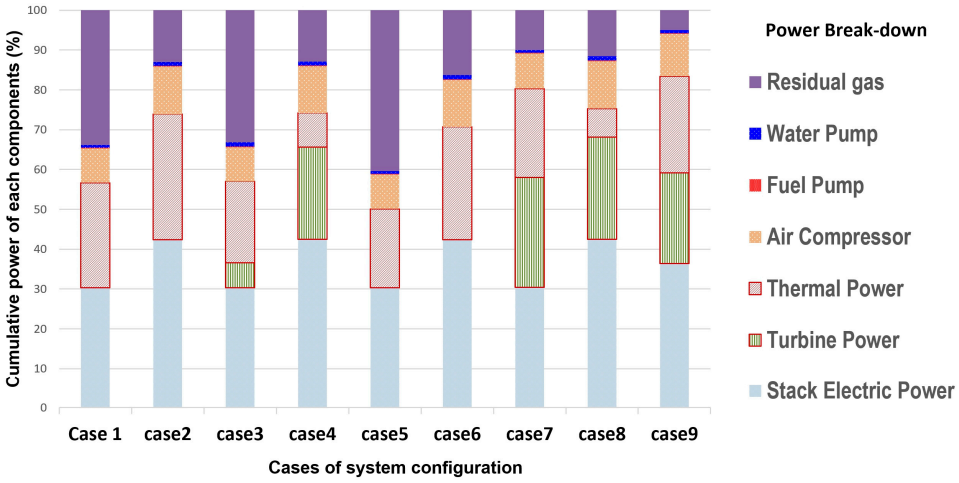

Figure 7. Cumulative power ratio from power source to parasitic power loss (%).

4. Conclusions

A feasibility study of the SOFC system with an external reformer has been conducted. Twelve different system layouts were analyzed, and the following is concluded:

1. When the external reforming SOFC used a conventional burner for heat supply to the reformer, the electrical efficiency of the SOFC system was 21.89% due to the additional fuel supply to the conventional burner. Additionally, the thermal power out was the lowest for all the analyzed system layouts. The additional fuel supply to the conventional burner could be removed when a catalytic combustor was applied, as in Case 2. Those cases show an improvement of 8.9% in electrical efficiency and 28% in thermal efficiency, compared with Case 1.
2. To enhance the reference system efficiency, the turbine utilization of waste thermal energy generated extra electricity, and the vortex tube improved the thermal energy usage. The systems of Case 3 and Case 4 installed the turbine with the SOFC. Consequently, the efficiency of the system adopting the catalytic combustor was the highest compared to the other cases, resulting in an improvement of 32.31% in the electrical efficiency and 23.75 % in the thermal efficiency. On the other hand, thermal energy utilization was confirmed in Case 5 and Case 6 when the SOFC was installed with a vortex tube. Even though thermal energy utilization improved, only a minor efficiency improvement was observed. On the other hand, when the system in Case 7 utilized the vortex tube to heat up the air supplied to the cathode, the layout improved electrical efficiency by 2.36% and thermal efficiency by 0.96%, compared with Case 4.
3. In Case 8, when a catalytic combustor was additionally adopted to increase turbine power, the electric efficiency decreased to 49.40% due to the additional fuel. Nevertheless, the thermal efficiency was shown to increase to 71.69%. When the secondary reformer, catalytic combustor, and turbine were installed in Case 9, the system reduced the additional fuel usage to 16.42% and increased the thermal efficiency to 85.92%.
4. As a whole, the temperature rise capability of the energy separation device helped to improve the system efficiency of the SOFC system.

Author Contributions: Conceptualization, Y.K. and E.-J.C.; investigation, J.Y.; writing—original draft preparation, J.Y. and E.-J.C.; writing—review and editing, E.-J.C.; supervision, S.Y.; project administration, S.L. All authors have read and agreed to the published version of the manuscript.

Funding: This research was funded by KEIT, grant number 20004963, and NRF, grant number NRF-2022R1A4A1030333.

Data Availability Statement: The data presented in this study are available on request from the corresponding author. The data are not publicly available due to privacy.

Acknowledgments: This work was supported by the Technology Innovation Program, funded by the Korea Evaluation Institute of Industrial Technology (KEIT), the Ministry of Trade, Industry and Energy (MOTIE) of the Republic of Korea (No. 20004963), and the National Research Foundation of Korea (NRF), grant funded by Korea Government (MSIT) (NRF-2022R1A4A1030333).

Conflicts of Interest: The authors declare no conflict of interest. The funders had no role in the design of the study; in the collection, analyses, or interpretation of data; in the writing of the manuscript; or in the decision to publish the results.

Nomenclature

Q	heat flow rate, W
n	mole flow rate, mol/s
J	current, A
F	faraday constant, C/mole
N	number of stacked fuel cell
U	utilization
p	pressure, kPa
P	power, W
LHV	lower heating value, kJ/kg
Cp	constant pressure specific heat, kJ/kg
Greek Letters	
γ	specific heat ratio
η	efficiency
λ	amount of excess air
Subscripts	
AC	alternative current power
DC	direct current power
sys	system
turb	turbine
f	fuel
h	hot flow
c	cold flow
is	isentropic
a	ambient

References

1. Wang, Y.; Wehrle, L.; Banerjee, A. Anlysis of a bio-fed SOFC CHP system based on multi-scale hierarchical modeling. *Renew. Energy* **2021**, *163*, 78–87. [CrossRef]
2. Fisavi, B.; Chitsaz, A.; Hosseinpour, J.; Ranjbar, F. Thermo-environmental and economic comparison of three different arrangements of solid oxide fuel cell-gas turbine (SOFC-GT) hybrid systems. *Energy Convers. Manag.* **2018**, *168*, 343–356.
3. Komatsu, Y.; Kimijima, S.; Szmyd, J.S. Performance analysis for the part-load operation of a solid oxide fuel cell-micro gas turbine hybrid system. *Energy* **2010**, *35*, 982–988. [CrossRef]
4. Khani, L.; Mahmoudi, S.M.S.; Chitsaz, A.; Rosen, M.R. Energy and exergoeconomic evaluation of a new power/cooling cogeneration system based on a solid oxide fuel cell. *Energy* **2016**, *94*, 64–77. [CrossRef]
5. Barelli, L.; Bidini, G.; Ottaviano, A. Integration of SOFC/GT hybrid systems in Micro-Grids. *Energy* **2017**, *118*, 716–728. [CrossRef]
6. Biert, L.V.; Godjevac, M.; Visser, K.; Aravind, P.V. Dynamic modelling of a direct internal reforming solid oxide fuel cell stack based on single cell experiments. *Appl. Energy* **2019**, *250*, 976–990. [CrossRef]
7. Badur, J.; Lemanski, M.; Kowalczyk, T.; Zioikowski, P.; Kornet, S. Zero-dimensional robust model of an SOFC with internal reforming for hybrid energy cycles. *Energy* **2018**, *158*, 128–138. [CrossRef]
8. Huber, T.; Opitz, A.; Kubicek, M.; Hutter, H.; Fleig, J. Temperature gradients in microelectrode measurements: Relevance and solutions for studies of SOFC electrode materials. *Solid State Ion.* **2014**, *268*, 82–93. [CrossRef]
9. Lee, T.H.; Choi, J.H.; Park, T.S.; Yoo, K.B.; Yoo, Y.S. Development of kW class SOFC systems for combined heat and power units at KEPRI. *J. Korean Ceram. Soc.* **2008**, *45*, 772–776. [CrossRef]
10. Agnew, G.D.; Bozzolo, M.; Moritz, R.R.; Berenyl, S. The design and integration of the Rolls-Royce fuel cell systems 1MW SOFC. *ASME Turbo Expo* **2005**, *2*, 801–806.
11. Becker, W.L.; Rraun, R.J.; Melaina, M. Design and the technoeconomic performance analysis of a 1MW solid oxide fuel cell polygeneration system for combined production of heat, hydrogen and power. *J. Power Source* **2012**, *200*, 34–44. [CrossRef]

12. Costamagna, P.; Selimovic, A.; Borghi, M.D.; Agnew, G. Electrochemical model of the integrated planar solid oxide fuel cell (IP-SOFC). *J. Chem. Eng.* **2004**, *102*, 61–69. [CrossRef]
13. Saebea, D.; Authayanun, S.; Patcharavorachot, Y. Use of different renewable fuels in a steam reformer integrated into a solid oxide fuel cell: Theoretical analysis and performance comparison. *Energy* **2013**, *51*, 305–313. [CrossRef]
14. Seabea, D.; Magistri, L.; Massardo, A. Cycle Analysis of Solid oxide fuel cell-gas turbine hybrid systems integrated ethanol steam reformer: Energy Management. *Energy* **2017**, *127*, 743–755. [CrossRef]
15. Ma, S.; Hu, X.; Zhao, Y.; Wang, X.; Dong, C. Design and Evaluation of a Metal-Supported Solid Oxide Fuel Cell Vehicle Power System with Bioethanol Onboard Reforming. *ACE Omega* **2021**, *6*, 29201–29214. [CrossRef]
16. Deng, M.; Liu, J.; Zhang, X.; Li, J.; Fu, L. Energy and parameter analysis of SOFC system for Hydrogen production for methane steam reforming. *J. Therm. Sci.* **2022**, *31*, 2088–2110. [CrossRef]
17. Braun, R.J.; Klein, S.A.; Reindl, D.T. Evaluation of system Layout for solid oxide fuel cell-based micro-combined heat and power generators in residential applications. *J. Power Sources* **2006**, *158*, 1290–1305. [CrossRef]
18. Ghang, T.G.; Yu, S.; Kim, Y.M.; Ahn, G.Y. Experimental study of steam reforming assisted by catalytic combustion in concentric annular reactor. *KSME J.* **2010**, *34*, 375–381. [CrossRef]
19. Hayes, R.E.; Kolaczkowski, S.T. *Introduction to Catalytic Combustion*; Gordon and Breach Science Publishers: London, UK, 1997; pp. 401–422.
20. Valipour, M.S.; Niazi, N. Experimental modeling of a curved Ranque-Hilsch vortex tube refrigerator. *J. Refrig.* **2011**, *34*, 1109–1116. [CrossRef]
21. Xue, Y.; Arjomandi, M.; Kelso, R. A critical review of temperature separation in a vortex tube. *Exp. Therm. Fluid Sci.* **2010**, *34*, 1367–1374. [CrossRef]
22. Dutta, T.; Sinhamahapatra, K.P.; Bandyopadhyay, S.S. Numerical investigation of gas species and energy separation in the Ranque-Hilsch vortex tube using real gas model. *J. Refrig.* **2011**, *34*, 2118–2128. [CrossRef]
23. Im, S.Y.; Yu, S. Effects of geometric parameters on the separated air flow temperature of a vortex tube for design optimization. *Energy* **2012**, *37*, 154–160. [CrossRef]
24. Hu, Z.; Li, R.; Yang, X.; Yang, M.; Day, R.; Wu, H. Energy separation for Ranque-Hilsch vortex tube: A short review. *Therm. Sci. Eng. Prog.* **2020**, *19*, 100559. [CrossRef]
25. Attalla, M.; Ahmed, H.; Ahmed, M.S.; El-wafa, A.A. Experimental investigation for thermal performance of series and parallel Ranque-Hilsch vortex tube systems. *Appl. Therm. Eng.* **2017**, *123*, 327–339. [CrossRef]

Disclaimer/Publisher's Note: The statements, opinions and data contained in all publications are solely those of the individual author(s) and contributor(s) and not of MDPI and/or the editor(s). MDPI and/or the editor(s) disclaim responsibility for any injury to people or property resulting from any ideas, methods, instructions or products referred to in the content.